Analytical and Experimental Observations of Ionospheric and Tropospheric Decorrelation Effects for Differential Satellite Navigation during Precision Approach

Jock R. I. Christie, Ping-Ya Ko§, Boris S. Pervan, Per K. Enge, J. David Powell, Bradford W. Parkinson

Department of Aeronautics and Astronautics
Stanford University

§Chung Shan Institute of Technology and Science

Abstract

The introduction of the Global Positioning System (GPS) ushered in a new era of affordable precise navigation. Differential GPS (DGPS) corrections have reduced positioning errors from about 100 meters to roughly 1 meter, which has led to their proposed use in aircraft precision approach. However, the accuracy of differential corrections is somewhat limited by spatial and temporal decorrelation of the atmosphere. Current requirements for precision landing, which limit integrity risk to one undetected navigation hazard in a billion trials, suggest that we must fully characterize ionospheric and tropospheric decorrelation. This paper will present both theoretical and experimental results in this regard.

Currently assumed values of spatial decorrelation for the ionosphere and troposphere are about 2 and 1 mm/km respectively. This suggests an error of only 2 centimeters error due to the ionosphere, and 1 centimeter error due to the troposphere at 10 kilometers from the DGPS reference station. However, these are simply average values based on relatively smooth models of the ionosphere and troposphere. These values seem overly optimistic when compared to a documented case of ionospheric decorrelation that resulted in a 50 centimeter difference between ionospheric estimates over a 9 kilometer baseline.

Models of the troposphere were also analyzed to examine the variability due to changing surface conditions. Archived inflight data from a prototype Local Area Augmentation System (LAAS) architecture was post processed using several different tropospheric models. Carrier phase residuals were calculated at each epoch as a measure of model consistency. The actual displacement due to a change in model was examined to determine the sensitivity to ground measurements of temperature, pressure and humidity.

The archived LAAS flight data was input to a Carrier Smoothed Code algorithm, along with an assumed ionospheric gradient. The impact of filter time constants on pseudorange error was calculated.

This paper seeks to obtain statistical bounds for the tropospheric and ionospheric decorrelation effects on a LAAS architecture.

Introduction

Measurement decorrelation is an issue for precision DGPS applications such as LAAS. Decorrelation is roughly linear with range from the reference station, thus it becomes less of a threat as you move farther from (and higher above) the airport. Previous GPS research in Antarctica measured a decorrelation of 50 cm over a 9 km baseline, all of which was attributed to the ionosphere [Goad]. This is equal to a decorrelation gradient of 55 mm/km, which is 20 times larger than the typical quoted values. While polar regions typically experience larger values of TEC, this single observation is still quite alarming since it is certainly not the worst possible point, just the worst one that was observed during the short campaign.

The dry component of tropospheric delay constitutes about 90% of the tropospheric delay and is fairly stable over periods of an hour or so. The wet component is smaller, but is much less stable - changing considerably over the course of an hour - or during a displacement of several kilometers.

The first half of this paper will address the tropospheric concerns, while the latter half focuses on the ionosphere.

MASPS Requirements

The RTCA has derived upper bounds for the residual errors due to DGPS for the Signal in Space (SIS). This model is given by the following equation:

$$1) \qquad \sigma_{res} \le \sqrt{a_2^2 + \left(\frac{a_3}{\sin\theta}\right)^2}$$

The residual error is composed of two distinct types of error source. The “a2” term is independent of elevation angle and contains errors due to SA (clocks), ephemeris, multipath, and receiver noise. However we are more concerned with the “a3” term which is due to the **zenith** delay of the troposphere and the ionosphere. Note that the obliquity correction built in to the equation is accurate for the troposphere, but probably

overstates the ionospheric error at low elevation angles. The following analyses will examine only the zenith delay for both the troposphere and the ionosphere, because the "a3" term is divided by the sin of the elevation angle.

The following table summarizes the specifications for the standard deviation at the decision height (h = 100 feet = 30.5 meters), and at the service ceiling (h = 1290 feet = 363 m)

TABLE 1.

		σ_{tropo}	σ_{iono}	σ_{total}
Cat I, II	DH = 61 m	20 mm	20 mm	30 mm
	CEIL = 393 m	130 mm	130 mm	185 mm
Cat III	DH = 30.5 m	7 mm	7 mm	10 mm
	CEIL = 393 m	91 mm	91 mm	130 mm

The MASPS specification states that requirements are proportional to the altitude, which results in a tapered "tunnel", much like was present with the ILS specifications.

We anticipate some spatial decorrelation of the correction due to inhomogeneities in both the troposphere and the ionosphere. The following analyses show that these decorrelations produce small errors relative to the DGPS corrections, and they are smaller than the specification on an epoch by epoch basis. However, carrier smoothing of GPS signals with ionospheric gradients will exhibit an error roughly equal to the ionospheric error that existed two time constants ago.

Troposphere - Assumptions

The analysis of tropospheric decorrelation makes the following assumptions:

• *Linear vertical temperature profile.*

This is a common and realistic assumption. The "Lapse Rate" is the vertical temperature gradient

$$2) \quad \beta = \frac{dT}{dh} \cong -7\frac{^\circ C}{km}$$

• *Slab model, uniform at a given height.*

This assumption is true in most cases for a moderate distance from the airport (r ≤ 10 km). Clearly this assumption is not true at longer distances or the local weather would never change. This assumption is clearly unrealistic if there are microclimates present, as happens in the San Francisco Bay Area. Unfortunately, measurements of this discrepancy are difficult and expensive. Previous research has examined the effect of weather fronts on GPS measurements [Gregorius]

Troposphere - Equations

$$3) \quad N = (n-1)\times 10^6 \cong 320$$

Typical values for the index of refraction are n ~ 1.00032 or N ~ 320. The delay can be calculated using the surface weather conditions as follows

$$4) \quad N = k_1\frac{P_{dry}}{T} + k_2\frac{P_{wet}}{T} + k_3\frac{P_{wet}}{T^2}$$

where the values of k are as follows

$$k_1 = 77.604\frac{K}{mb} \pm 0.02\%$$

$$5) \quad k_2 = 75\frac{K}{mb} \pm 10\%$$

$$k_3 = 375000\frac{K^2}{mb} \pm 1\%$$

It has been suggested [Clynch] that $k_2 = 0$. This is reasonable since there is a lot of uncertainty in k_2, and the magnitude of the second term is typically less than 5% of magnitude of the third term. This assumption will be used from now on.

The wet pressure is a function of dewpoint temperature (T_d) or relative humidity; it can be calculated as follows.

$$6) \quad P_{wet}(T_d) = e^{\frac{L}{R_v}\bullet\left(\frac{1}{273.15}-\frac{1}{T_d}\right)} \bullet 6.11mb$$

Where L/R_v = 2.5E6/461 = 5422 K. Assuming sea level pressure conditions of 1015 mb and a temperature of 20 °C (293.15 K), *Equation 6)* yields wet pressure values ranging from 0.0 mb (RH = 0%) to 23.7 mb (RH = 100%). *Equation 4)* yields N from 262 to 365 as the relative humidity increases from 0% to 100%. Because colder air can hold much less water vapor, this variation in N is reduced in colder climates. Specifically, if the temperature is 0 °C (273.15 K), then the maximum wet pressure is 6.1 mb and N varies from 267 to 293, depending on humidity.

Sensitivity Analysis

Equation 4) and *Equation 6)* were combined and then a Taylor Series approximation was made to determine the sensitivity of N to ground measurements.

$$7) \quad \Delta N = \left(\frac{\partial N}{\partial T}\right)\Delta T + \left(\frac{\partial N}{\partial T_d}\right)\Delta T_d + \left(\frac{\partial N}{\partial P}\right)\Delta P$$

$$\frac{\partial N}{\partial T} = -1 \bullet \left(k_1 \frac{P_{dry}}{T^2} + k_2 \frac{P_{wet}}{T^2} + 2k_3 \frac{P_{wet}}{T^3} \right)$$

8) $$\frac{\partial N}{\partial T_d} = \left(\frac{L/R_v}{T^2} \right) P_{wet} \left(-\frac{k_1}{T} + \frac{k_2}{T} + \frac{k_3}{T^2} \right)$$

$$\frac{\partial N}{\partial P} = \frac{k_1}{T}$$

Evaluating the expressions in *Equation 8)* at typical conditions of T = 20.0 °C, T_{dew} = 15.0 °C (RH = 72.1%), and P = 1013 mb, N = 338

9) $$\Delta N = \left(\frac{-1.4}{K} \right) \Delta T + \left(\frac{4.6}{K} \right) \Delta T_d + \left(\frac{0.3}{mb} \right) \Delta P$$

Alternatively, we could write

10) $$\Delta N = -410 \frac{\Delta T}{T} + 1325 \frac{\Delta T_d}{T_d} + 304 \frac{\Delta P}{P}$$

Thus a 1% change in Dew Point (Δt_d = 2.83°C) leads to a ΔN = 13.2, which is roughly 4% change. This shows that for these particular conditions (and coefficients), the variation in N is most sensitive to variations in the dew point. In most cases, the dew point varies much less during the course of a day than the temperature does, particularly in desert areas.

Pseudorange correction due to Troposphere

11) $$\Delta\tau = \int \left(\frac{1}{v} - \frac{1}{c} \right) dl = \frac{1}{c} \bullet \int (n-1) dl = \frac{10^{-6}}{c} \bullet \int N(h) dl$$

This value of Δτ is the delay in seconds. This can be expressed as the delay in meters, which is what is observed in the pseudorange domain. The altitude and the path length inside the troposphere are given by $h = l \sin\theta$. Thus the pseudorange correction can be estimated as

12) $$\Delta R = c\Delta\tau = \frac{10^{-6}}{\sin\theta} \bullet \int N(h) dh$$

This equation is similar in form to the one shown earlier as part of the MASPS requirements. The $\sin\theta$ in the denominator converts from zenith delay to slant delay, and will be omitted from now on.

The following equation relates the model error in N to the resulting zenith pseudorange delay.

13) $$\Delta PR = 10^{-6} (\Delta N) H$$

This equation can be rewritten to find the variation in refractivity that would be necessary to produce and error of 7 millimeters at the decision height of 30 meters.

14) $$\sigma N_{DH} = 10^6 \frac{\sigma PR_{DH}}{H_{DH}} = 10^6 \frac{0.007m}{30m} = 233$$

The resulting value of 233 units of N is approximately 70% of the nominal value of N (roughly 320). We will now try to determine the variability (standard deviation) in refractivity.

Troposphere: Weather Data

The National Oceanic and Atmospheric Administration (NOAA) maintains historical weather data for hundreds of airport all over the country. Some of these archives begin over 100 years ago. A small portion of this data was examined to determine the variability in surface conditions. While this data was very useful in understanding the surface conditions and their temporal variation, it does not provide any knowledge about the tropospheric profile an aircraft might observe while landing.

The first set of meteorological data that was analyzed contained daily mean, high, and low temperatures, as well as average dewpoint, and average pressure. Refractivity was calculated for each day in the two year archive. The mean value of N for these two years was 320.0

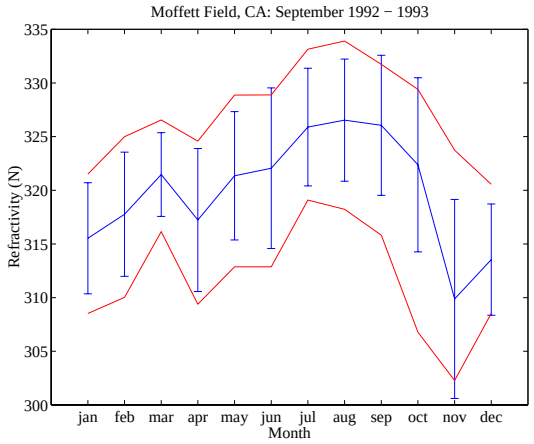

Figure 1 **Monthly Means at Moffett**
Two years of data was averaged to find mean refractivity for each month.

Flight Tests

A series of flight tests were conducted in September 1997 at Moffett Field California, part of the NASA Ames Research Center. The purpose of these tests was to test and evaluate a prototype LAAS architecture that had been developed at Stanford [Pervan]. The archived flight data can be

postprocessed to examine the effect of various tropospheric models and coefficients.

The Flight Service Station at Moffett Field provided hourly measurements of temperature, dewpoint, and pressure. From these values, N was calculated, and a histogram of N is shown below.

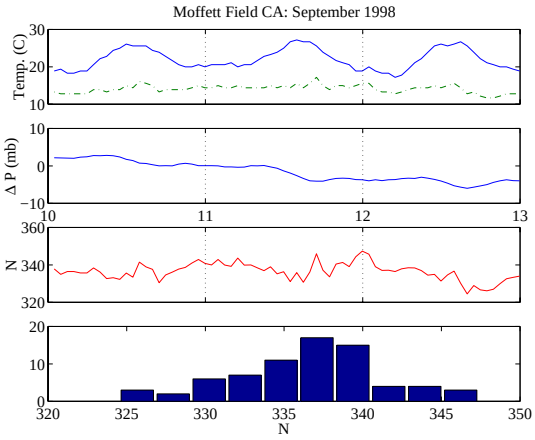

Figure 2 Hourly Weather at Moffett
Hourly record of Temperature and Dewpoint, Pressure, and calculated values of Refractivity, for 3 days in September 1997

The standard deviation observed in this small data set was 4.6, which is equivalent to 0.1 mm of error at the decision height.

During the flight tests, we recorded continuous carrier phase measurements for post processing, and as a sort of truth measurement. By using the static preflight survey, it is possible to resolve cycle ambiguities and achieve position errors on the order of 1 cm. An important measure of this error is the normalized residuals that remain after solving for our position in the least squares sense.

We would expect that all error sources would increase as we get further from the reference station. We believe that the primary error source over these short baseline (less than 10 km) is due to the troposphere.

Figure 3 shows the bird's-eye view of the pattern flown at Moffett on a typical day. A counterclockwise approach was flown to runway 32Left. In some cases, the base leg was over 25 km from the airport, so the data was limited to just those points on the 3° glide slope and within 12 km of the airport.

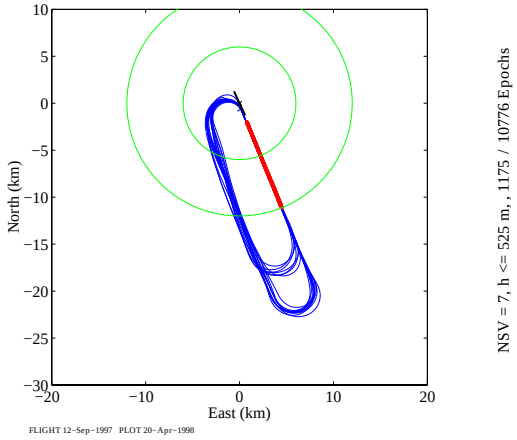

Figure 3 Overhead view of LAAS flight path
The 2D projection of several flight trials on a North-East grid.

*Figure 4*shows the normalized residual as a function of elevation. A least squares line was fit to the mean. The observed trend increases with altitude as expected. The residuals are scaled in such a way that any value greater than 0.5 suggests a systematic error in estimating the integers. All values of the residual are clustered below 0.2 units

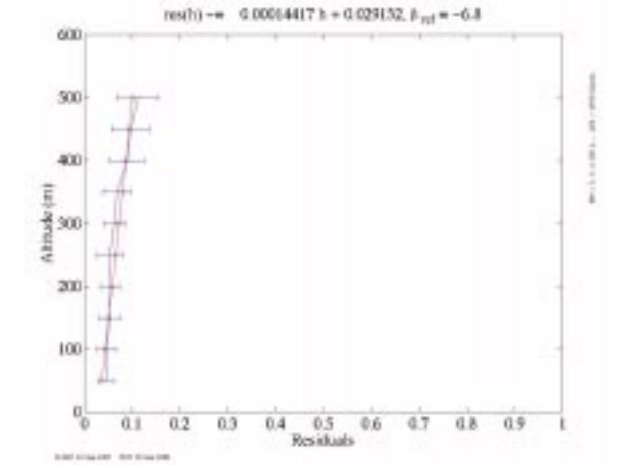

Figure 4 Normalized Residual vs. Altitude
The mean and standard deviation of the normalized residual is plotted in 10 vertical bins

National Weather Data

The preceding sets of weather data were exclusively focused on our test airport, Moffett Field. It is important to

make sure that our findings at Moffett are representative of the entire nation.

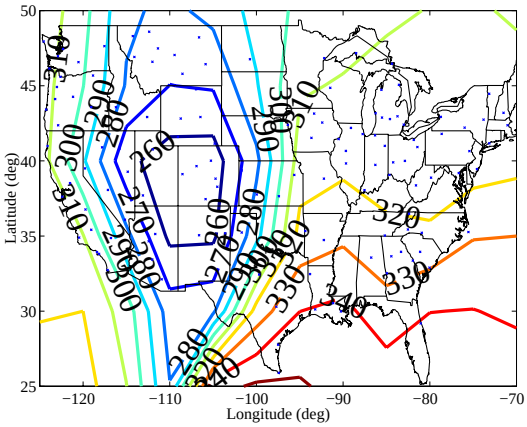

Figure 5 **Average Refractivity for one Year**
This mean refractivity was calculated at 134 airports and passed through a grid algorithm.

Figure 5 shows that the refractivity (N) is consistently higher at lower latitudes. At first this seems counterintuitive, since lower latitudes are associated with higher temperatures and thus lower values of N. However, it is the second and third term in *Equation 4)* that includes the effect of higher humidity.

The reduced values of N over the Rocky Mountains are readily observable on this plot. N was calculated using the surface measurements, without correcting for altitude. Thus the lower pressures at higher elevations reduced the refractivity substantially.

During this fairly typical year the mean refractivity of all sites for all days was N = 303. The annual mean value for any one site ranged from a low of N = 207 to a high of N = 394.

The steep gradient in N that occurs in central Texas clearly shows that significant change in weather can accompany changes in lateral position. This would be a concern if this large change in N were observed over a shorter baseline and could thus produce different conditions for an approaching aircraft than were observed at the ground reference station.

While a mean value of N = 303 is good enough for all CONUS airports, it is relatively easy to calculate the *local* mean and use that for every airport, further reducing a small error source.

Ionosphere

Differential ionosphere delay is the path length difference between the ground reference station (the Ground) and the aircraft (the Air) when the satellite signal penetrates through the ionosphere. This error source has previously been ignored by assuming that the ionosphere spatial decorrelation for LAAS users is negligible due to the fact that the Air and the Ground are physically close to each other. However, the effect of the officially selected Carrier Smoothed Code (CSC) on the differential ionosphere delay has not been studied yet. Therefore, the purpose here is to characterize the effect of the differential carrier smoothed ionosphere delay on LAAS.

Previous research showed several observed ionosphere spatial decorrelation for the local area Differential GPS (DGPS) as described in the following but none of them discussed the differential carrier smoothed ionosphere delay. *Goad[1990]* observed 0.5m slant differential ionosphere error over 9km baseline in antarctica during the last solar maximum period. *Wanninger[1993]* recorded a 5m gradient of the ionosphere over a 100km baseline in Brazil during the last solar maximum period. *Warnant[1997]* presented that Travelling Ionospheric Disturbances (TID) could cause severe ionosphere gradient over a 15 to 20km baseline and will limit geodetic applications of DGPS. *Doherty[1997]* reported a 0.7m/min temporal vertical ionosphere gradient in the evening at Fairbanks, AK., in a solar moderate period. These observed ionosphere gradients are useful reference for the study of the differential carrier smoothed ionosphere delay.

Differential Ionosphere Delay

Differential ionosphere delay is the spatial decorrelation of the ionosphere between the Ground and the Air as the ΔI_0 shown in *Figure 6*.

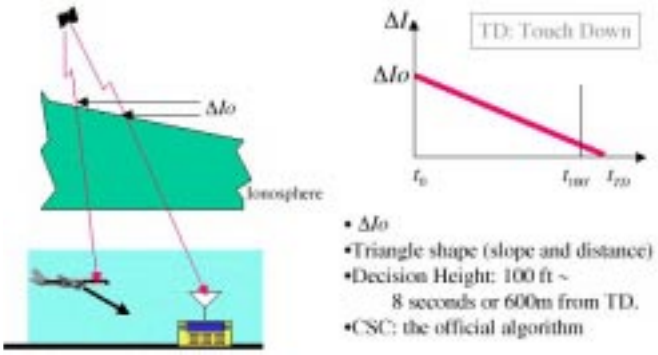

Figure 6 **Differential Ionosphere Delay**

For an approach, the Initial Approach Fix is made at roughly 54 km (30 nautical miles), which corresponds to t_0 in the right half of *Figure 6*. As the airplane approaches the runway, the spatial decorrelation of the ionosphere becomes smaller and smaller. When the airplane touches down, there is *no* spatial decorrelation at all which means that the differential ionosphere delay is zero. Therefore, the time histogram of the ΔI_0 looks like a triangle as shown in the right half of *Figure 6*.

For CAT III landings, the requirement is to check the CAT III availability at the DH of a 30.5 meters (100ft), it's about 600 m from TD, where the spatial decorrelation is less than several centimeters and should not be a problem. Therefore, neglecting the differential ionosphere delay has been the assumption in the LAAS application for a long time.

Currently, LAAS has selected the CSC as the official signal processing algorithm. The CSC is applied individually to the Ground and the Air. The Air receives the carrier

smoothed correction sent out from the Ground and subtract it from the Air's carrier smoothed pseudorange for positioning. Therefore, the differential ionosphere effect has transformed into a differential carrier smoothed ionosphere delay.

Carrier Smoothed Multipath

Multipath data collected during the flight tests at Moffett Field is shown below in *Figure 7*. The upper plot shows the airborne multipath versus time. The bottom panel shows the carrier smoothed multipath versus time with different time constants. We can clearly see that the CSC significantly reduces the multipath as the time constant increases. The filtering of noisy data is the primary advantage of using CSC.

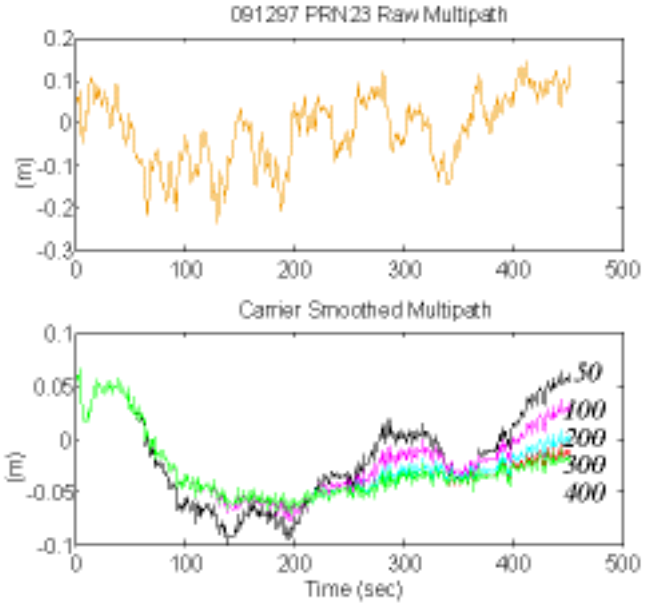

Figure 7 Carrier Smoothed Multipath
Sample flight data from Moffett field, with and without filtering.

Differential Carrier Smoothed Ionosphere Delay

The sample data from *Figure 7* was combined with a severe case ionosphere gradient. This data was then passed through the CSC algorithm, and the resulting differential carrier smoothed ionosphere delay is shown in *Figure 8*. It shows the differential carrier smoothed ionosphere delay versus time with different carrier smoothing time constants. The 0.8m differential ionosphere error over a 30km baseline is worse than the average but less than the worst. The lowest line is the unsmoothed differential ionosphere delay with multipath. Here we can clearly see the problem. The CSC delays the differential ionosphere effect on the LAAS. The longer the time constant, the worse the delay. For the most popular carrier smoothing time constant of a 100 seconds, at the DH of 30.5 meters (100 ft), the differential ionosphere error has been pumped up from less than 1 centimeter to about 40 centimeters. It is a large value when we compare it with the one sigma value of 10 to 15 centimeters of the carrier smoothed multipath. Therefore, to prevent from this delayed ionosphere error, we prefer a shorter carrier smoothing time constant.

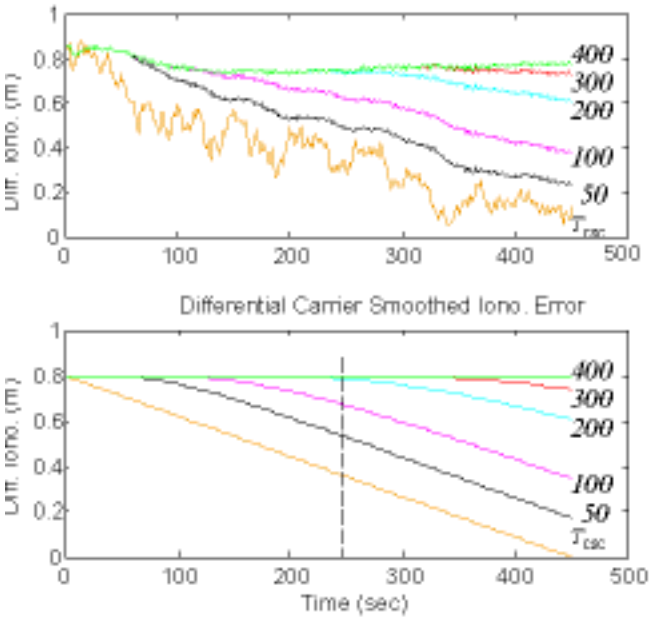

Figure 8 Differential Carrier Smoothed Ionosphere Delay

How big is the time delay due to the CSC? A detailed formula will be given in a later section. For now, we can roughly estimate from *Figure 8* there is a time delay of about twice the carrier smoothing time constant. Due to this time delay, the equivalent spatial separation now is the distance at the DH of 30 meters (100 ft) plus twice the carrier smoothing time constant times the airplane's velocity that is approximately 15km for the case of 100 seconds carrier smoothing time constant.

As we can see above, the carrier smoothed ionosphere delay and the carrier smoothed multipath, we have opposite requirements (divergence) on the carrier smoothing time constant that deserves further study.

To have more insights of the differential carrier smoothed ionosphere delay, let's start with the ionosphere model.

Ionosphere Model

The ionosphere is modeled as a thin slab at a height of 350km above the reference geoid as shown in *Figure 9*. The obliquity factor (Ob) is defined as the ratio of the measured slant delay over the vertical delay. Ob is a function of the satellite elevation as shown in the right top figure. It varies from about 3 at low elevations to 1 near the zenith.

For the differential ionosphere, we are concerned with two things: the distance between the Ionosphere Pierce Points

(IPP) of the Ground and the Air as the Δl_{IPP} shown in the left figure and the vertical spatial gradient.

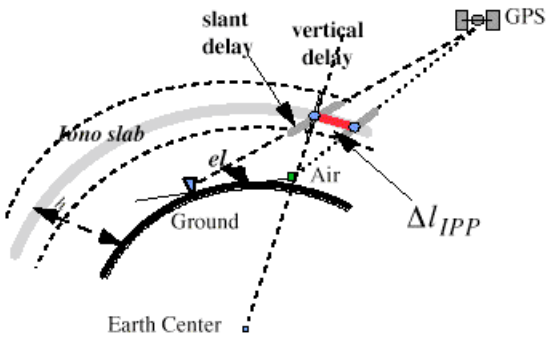

Figure 9 Ionosphere Model

In the 2-D case, the IPP distance is a function of the satellite elevation (el) and is proportional to the baseline distance (shown as R_0). The variation of the unit baseline IPP distance $\Delta l_{IPP,u}$ versus elevation ranges from 0 when the satellite is near the horizon to almost 1 when the satellite is near the zenith.

Since we assumed that the ionosphere changes slowly, the longitudinal spatial gradient could be approximated by the slope of the measured vertical ionosphere delay as shown in *Figure 10*. For the latitudinal spatial gradient, aligned latitudinal reference stations are needed to take measurements.

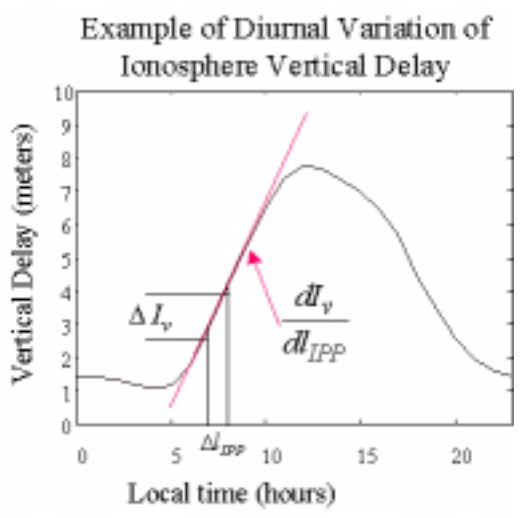

Figure 10 Spatial Gradient
Typical ionospheric spatial gradient, showing peak change rate in the late morning.

The 2-D differential (slant) ionosphere delay, can be derived from *Figure 10*. The (slant) delay can be approximated by the product of the spatial gradient, the Geometry Factor and the baseline, where the Geometry Factor is defined as $Ob\Delta l_{IPP,u}$

$$15) \quad \Delta I = I_a - I_g \approx \frac{dI_v}{dl_{IPP}} Ob\Delta l_{IPP,u} R_0$$

IPP Distance & Geometry Factor

The 2-D analysis can be extended into the real (3-D) world. The unit IPP distance ($\Delta l_{IPP,u}$) versus the azimuth and the elevation angles of a satellite is shown below in *Figure 11*.

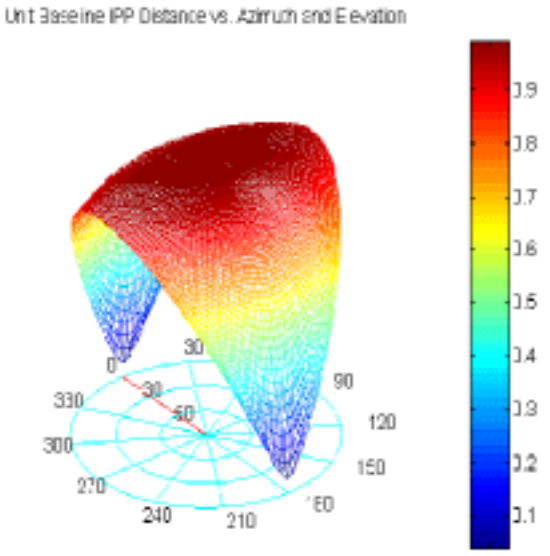

Figure 11 3-D Unit baseline IPP distance
Normalized IPP distance as a function of satellite azimuth and elevation.

When the satellite is along the (red) baseline (azimuth ~ 0° or 180°), $\Delta l_{IPP,u}$ varies from zero at low elevations, to almost one at the zenith, like the 2-D results. When the satellite is perpendicular to the baseline (azimuth ~ 90° or 270°), the unit IPP distance is almost one for all elevation angles.

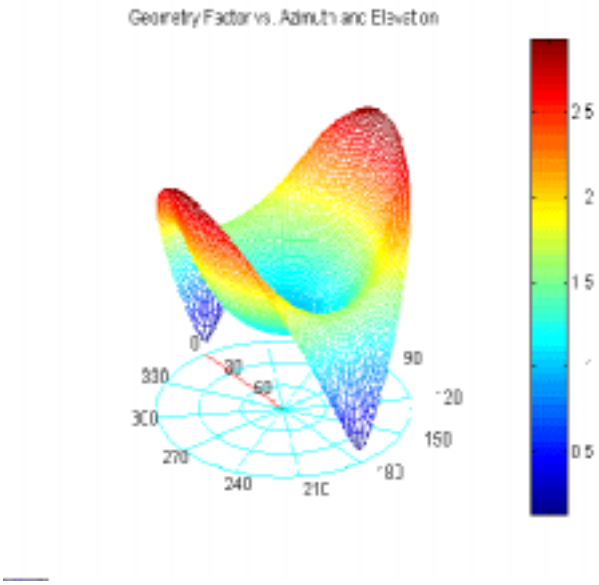

Figure 12 3-D Geometry Factor
Geometry factor ($Ob\Delta l_{IPP,u}$) as a function of satellite azimuth and elevation.

The geometry factor as we defined previously is shown in *Figure 12*. The geometry factor represents the sensitivity to spatial gradients in the ionosphere.

As we can see, the magnification due to the geometry factor can be as much as 2.8 which is significant. It means if the ionosphere gradient is along the baseline vector and the satellite is across the baseline at low elevation, then the differential carrier smoothed ionosphere delay will be 2.8 times the ionosphere gradient times the baseline. For the Wanninger's case, the ionosphere gradient is about 0.05m/km, and the baseline as mentioned above is about 15km, the differential carrier smoothed ionosphere delay could be 2.1 meters in the range domain. Remember this is the result for the carrier smoothing time constant of one hundred seconds. For longer time constant as widely discussed in the LAAS community, the effect of the differential carrier smoothed ionosphere delay will be more severe. We can no longer ignore the differential carrier smoothed ionosphere delay comparing to the carrier smoothed multipath error of about 10 to 15 centimeters.

Analytical Expression of the Differential Carrier Smoothed Ionosphere Delay

For the complete analysis of the effect of the differential carrier smoothed ionosphere delay on LAAS, an analytical expression of the differential carrier smoothed ionosphere delay was derived as shown in the following.

$$\Delta I(t, x) = I_{\hat{a}} - I_g \approx Ob\left\{2(\tau_a - \tau_g)\frac{\partial I_v}{\partial t}\bigg|_t\right\} + Ob\left\{[x + 2(\tau_a - T_s)v]\frac{\partial I_v}{\partial x_{IPP}}\bigg|_t \frac{\partial x_{IPP}}{\partial x}\right\} \quad 16)$$

where

t = Time

$x = R_0$ = Range or Position

$I_{a,g}$ = Ionosphere after CSC

Ob = Obliquity

$\tau_{a,g}$ = CSC Time Constant

I_v = Vertical Ionspheric Delay

x_{IPP} = Distance between the two IPPs

T_s = Sampling Interval

v = Velocity of Air wrt Ground

The assumptions made for the derivation of *Equation 16)* include:

- Assumed that the ionosphere varies slowly in time and space. Therefore, the temporal and the spatial gradients of both the carrier smoothed and the unsmoothed ionosphere delays are the same.

- Assumed that the temporal variation of the ionosphere delay in a local area is the same for both the Ground and the Air.

Equation 16) manifests both the temporal and spatial gradients affect the performance of LAAS.

- Temporal gradient will show up when the carrier smoothing time constants of the ground and the air are different. This provides an additional trade-off when considering different time constants for the Air and the Ground.

- The spatial gradient is multiplied by the *sum* of the baseline vector and the *product* of twice the Air's carrier smoothing time constant times the Aircraft velocity. The second term in*Equation 16)* is similar to the 2-D case of *Equation 15)*.

- This analytical expression is a very useful tool for the detailed analysis of the effect of the differential carrier smoothed ionosphere delay on the LAAS availability that requires further analysis.

Summary

- Zenith tropospheric errors seem to be quite small (< 7 mm) in all cases when at an elevation of 30 meters. These errors do grow with elevation, but the requirements are proportional to elevation, so there does not appear to be an integrity threat at any altitude.

- Discovered an error source due to the CSC filtering of the ionosphere that was previously ignored. It could significantly effect the availability of a LAAS-based landing system
  - » Differential carrier smoothed ionosphere delay is not negligible and its effect on the LAAS availability needs further study.
- Provided an analytical expression of the differential carrier smoothed ionosphere delay. It shows that
  - » using different carrier smoothing time constants for the Ground and the Air
  - » using larger carrier smoothing time constant for the Air

  will worsen the differential ionosphere effect.
- Provided an important tool for further availability analysis.

Conclusions

Both the troposphere and the ionosphere can produce small decorrelation errors when the aircraft (user) is several kilometers from the DGPS reference station. These errors are fairly small relative to the precision of a code based DGPS system and are therefore essentially negligible. The use of Carrier Smoothed Code can significantly increase the magnitude of the ionospheric error at the touchdown point. The ground and air must use equal time constants in the smoothing algorithm.

However, these same small errors are a large part of the error budget for a carrier phase DGPS. In particular, the divergent nature of the ionosphere leads to erratic results when using carrier smoothed code.

References

[BB] Global Positioning System, Theory and Applications, edited by Parkinson and Spilker, AIAA Washington DC

[Clynch] Clynch, J., Note to RTCA

{Doherty] Doherty, Patricia H. et al. "Spatial and temporal variations in ionospheric range delay", ION GPS-97, Kansas City, MO, USA., September 1997

[Goad] Goad, Clyde C., “Optimal filtering of pseudoranges and phases from single-frequency GPS receivers”, *Navigation*, Vol. 37, No. 3, Fall 1990

[Gregorius] Gregorius, Thierry, and Geoffrey Blewitt, “The Effect of Weather Fronts on GPS Measurements”, GPS World, May 1998

[Griffith] Griffith, Cheryl, Stephen Peck, Juan Ceva, and Rajendra Malla, "Should WAAS get Ride of the MET Instruments", ION January 1997

[Pervan] Pervan, Lawrence et. al., "Flight Test Evaluation of an Alternative Local Area Augmentation System Architecture", *Navigation*, Vol. 45, No. 2, Summer 1998

[Wanninger] Lambert Wanninger, Gunter Seeber, and Milton A. Campos, 'Limitations of GPS in Central and South America Due to The Ionosphere', presented at the Int. Conference "Cartography - Geodesy", Maracaibo, Venezuela, Nov 24 - Dec 4, 1992.

[Warnant] Warnant, René, "Influence of the ionospheric refraction on the repeatability of distances computed by GPS", ION GPS-97., Kansas City, MO, USA., September 1997

Acknowledgments

We would like to thank the FAA for their ongoing support of GPS research at Stanford University. We would also like to thank Donghai Dai, Sam Pullen, and Professor David Powell

Stanford GPS Lab
Stanford, CA 94305-4085

http://www.stanford.edu/group/GPS